Calibration chamber investigation into effect of confining pressure on mechanisms of compaction grouting

Effet de pression latérale sur les mécanismes de compactage solide dans la chamber d'étalonnage

A.M. El-Kelesh
Construction Engineering and Utilities Department, Zagazig University, Egypt
T. Matsui
Department of Civil Engineering, Ritsumeikan University, Japan
K. Tokida
Department of Civil Engineering, Osaka University, Japan

ABSTRACT
Compaction grouting has some problems that are basically attributed to the little understanding of grouting mechanisms. Large-scale double-wall calibration chamber and injection systems have recently been developed to physically model and investigate the technique in the laboratory. This paper describes the main features of the developed systems and presents and discusses results of injections performed into sand samples under different confining pressures. The grouting mechanisms are discussed in terms of the variation with injection of the vertical displacement of soil surface, the volume change of soil, and the coefficient of earth pressure at rest (K_0). The results and discussions reveal that during injection the soil exhibits large deformations and increases in the lateral stress. After termination or during suspension of injection, the soil experiences creep deformation and lateral stress relaxation. The initial stress condition of soil highly influences the soil deformation. The soil volume change increases with injection, but at an attenuating rate. A unique relationship between the increase of K_0 with injection and the volume of injected grout is established.

RÉSUMÉ
Le compactage solide a des problèmes qui sont attribués fondamentalement à peu de compréhension des mécanismes d'injection. Les systèmes de chambre d'étalonnage avec deux parois à grande échelle ont été developpés récemment, pour modeler physiquement et examiner le technique dans le laboratoire. Cet article décrit les caractéristiques principals des systèmes dévelopés et presente et discute les résultats d'injections réalisés sur les specimens de sable sous des pressions latérales differentes. Les mécanismes d'injection sont discutés en termes de la variation avec l'injection de désplacement verticale à la surface de sol, changement de volume de sol, et coefficient de pression des terres au repos (K_0). Les résultats et discussions révéllent que lors d'injection le sol expose déformation grande, augmentant la contrainte latérale. Après l'interruption ou lors d'injection, le sol connaît déformation de fluage et relaxation de contrainte latérale. La condition des contraintes initiales de sol influence déformation de sol beaucoup de bien, qui augmente par l'injection, mais à une vitesse atténuante. Un rapport unique entre l'augmente de K_0 par l'injection et le volume d'injection est établi.

Keywords: Calibration chamber, compaction grouting, creep, lateral stress, physical modeling, soil deformation, stress relaxation.

1 INTRODUCTION

Compaction grouting involves the injection of stiff grout that does not enter the soil pores but increases in size and displaces the surrounding soil through a distinct grout-soil interface. This provides for controlled treatment and renders the method effective in improving *in-situ* loose soils. The conventional design approach of compaction grouting assumes that the soil volume change due to grouting equals the volume of injected grout. It does not account for the effects of the soil properties and grouting conditions on the improvement. Based on this approach, the obtained improvements appear inconsistent with the predicted ones (e.g., Baker 1985; Boulanger & Hayden 1995). The problem is attributed basically to the little understanding of the grouting mechanisms.

Large-scale double-wall calibration chamber and injection systems have recently been developed to physically model and investigate the mechanisms of compaction grouting in the laboratory under well-controlled conditions. Using these systems, samples are prepared and consolidated and injections are performed under conditions approximating the actual in-situ conditions. The main features of these systems are described in this paper. Also, presented in the paper are the results of injections performed into sand samples under different confining stresses. These results are used to discuss the grouting mechanisms in terms of the variation with injection of the soil deformation, the soil volume change and the coefficient of earth pressure at rest (K_0).

2 EXPERIMENTAL SETUP AND PROCEDURE

The developed calibration chamber is of the double-wall type and has several innovative features that provide for preparing, consolidating and testing soils under conditions approximating the *in-situ* ones. A detailed description of the chamber components and controls and a comparison with previously developed largest double-wall chambers (in terms of size, boundary conditions, stress application, allowance for sample surface upheave and reaction to vertical stress) are presented by El-Kelesh & Matsui (2008). As shown in Fig. 1, the chamber consists of seven major components: base, piston, side membrane, double-wall barrel, retaining cylinder, lid and assembly rods. The chamber houses samples of 1.40 m in diameter and 1.45 m in height. Maximum working vertical and lateral stresses of 0.5 and 1.0 MPa, respectively, can be applied. The vertical stress is applied at the top of the sample via the piston by pressurized air, while the lateral stress is applied by water filling the annular space between the side membrane and the barrel.

The double-wall barrel is utilized to control the K_0-condition and impose different boundary conditions. The annular space between the sample and the inner wall (inner cell) as well as that between the inner and outer walls (outer cell) are filled with de-aired water. On increasing the vertical stress, the pressure of the inner cell increases due to the tendency of the sample to deform laterally. An electro-pneumatic (E/P) regulator is used to control the pressure of the outer cell and keep it constantly equal to the developed pressure of the inner cell. This control

Proceedings of the 17th International Conference on Soil Mechanics and Geotechnical Engineering
M. Hamza et al. (Eds.)

doi:10.3233/978-1-60750-031-5-19

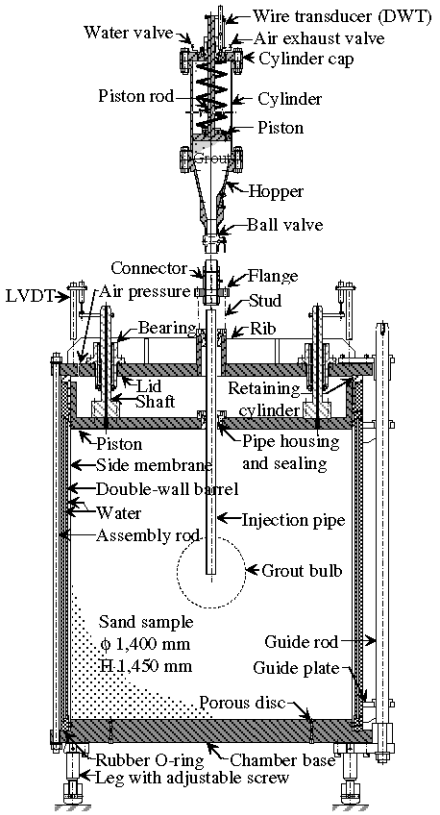

Figure 1. Setup of calibration chamber and injection pump.

assures no deflection of the inner wall, and thus zero average lateral deformation of the sample. The vertical stress and the lateral stress and strain can be independently controlled. The boundary conditions BC1 (constant vertical stress and constant lateral stress) and BC3 (constant vertical stress and zero lateral strain) provide good approximation of the free field conditions and are commonly used in calibration chamber testing (e.g., Parkin & Lunne 1982; Salgado et al. 1998). The chamber panel of controls can impose these boundary conditions.

The chamber utilizes a carefully designed vertical sliding system consisting of four shafts fixed to the piston and slide through linear bearings bolted to the lid. This system provides for sample compression up to 125 mm and upheave up to 25 mm from the initial sample surface. It also allows for externally measuring the displacement of the sample surface through the sliding shafts and four LVDTs. The piston slides through a rubber O-ring recessed in an annular shoulder machined in the inside of the barrel. The retaining cylinder is used to firmly retain this O-ring in position during movement of the piston and under the pressure differential (between the vertical air pressure and the lateral water pressure of the inner cell).

The developed injection system and its design challenges are described in detail by El-Kelesh & Mastui (2008). It consists of grout pump, water pump and a specially-designed connector. As shown in Fig. 1, the grout pump consists of cylinder with hopper, piston and cylinder cap. The pump cylinder is 200 mm in ID and permits a full piston stroke of 704 mm, and as a result continuous injection of 22.0 L of grout. The connector is used to connect the grout pump to the in-chamber injection pipe. The connector and the pipe setting are shown in Fig. 1; the pipe passes through central holes in the lid and piston. It is 50.8 mm in OD. Both the pipe and the connector have an ID of 44.8 mm. Six stud-bolts are used to fix the connector to the pipe. The pump piston is pressurized by supplying water under pressure by means of the water pump into the space between the piston and the cylinder cap. This results in the extrusion of the grout from the pump hopper and subsequently from the injection pipe. The water pump can apply pressures up to 5.0 MPa and deliver at rates up to 10.0 L/minute.

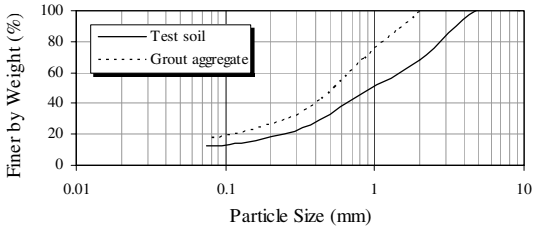

Figure 2. Gradations of test soil and aggregate of grout.

The test is conducted in five stages: sample preparation, chamber assembly, sample consolidation, injection and chamber disassembly. Uniform sand samples are prepared inside the rubber membrane (after being stretched inside a split former) by pluvial deposition through air. The relative density is controlled by varying the falling height of sand. After filling the former, the chamber piston is gently lowered on the top of sand and the membrane is sealed against the piston by means of metallic O-rings. Vacuum is applied to the sample and the former is disconnected. The chamber is then assembled around the sample, connected to the panel of controls and filled with de-aired water. After releasing the vacuum, the sample is K_0-consolidated to the desired stress. The grout pump is then filled with grout and connected to the injection pipe. The water pump is set to the desired injection rate and injection is started. After hardening of the injected grout, the chamber is disassembled.

3 RESULTS

In this paper, the results of four test cases are presented. The test soil is air-dried natural sand, the gradation of which is shown in Fig. 2. The specific gravity, maximum void ratio and minimum void ratio of the sand are 2.650, 0.923 and 0.562, respectively. The sand was deposited at a relative density of about 50%. Consolidation stresses (σ_v) of 0.085, 0.125, 0.165 and 0.205 MPa were considered for the four cases. These stresses, the lateral stresses (σ_h) at the end of consolidation and the relative densities are summarized in Table 1.

The injection process was volume-controlled and performed under the boundary condition BC3. The bulbs were injected at the mid-height of the sample. For Cases-1 and 3 three pump strokes were considered, while two strokes were considered for Cases-2 and 4. The suspension time (between each successive stroke) was 50–55 minutes. The grout was a mixture of fines-containing aggregate, cement, bentonite and water. The gradation of aggregate is shown in Fig. 2. The cement to aggregate and bentonite to aggregate ratios were 0.120 and 0.025, respectively. The grout slump (4.5 to 5.5 cm) and volume per stroke are shown in Table 1. An injection rate of 5.0 L/minute was considered.

Figure 3 shows the injection results of Cas-2, for example. They are represented as the variation with time (during injection and suspension) of the pump piston displacement (which is proportional to the volume of injected grout), the soil vertical and lateral stresses (the double-wall pressure which is the water pressure of the outer cell is also shown), and the vertical displacement of soil surface (as measured by the four LVDTs). The initial values shown in the figure are those attained at the end of consolidation and before starting injection. It is seen that the E/P regulator was satisfactorily responding to the changes in the lateral stress; the double-wall pressure was almost

Table 1. Characteristics of test cases.

Case	D_r	σ_v	σ_h		Grout Volume (L)			Slump
No.	(%)	(MPa)	(MPa)	K_0	S-1	S-2	S-3	(cm)
1	49	0.085	0.042	0.494	19.8	19.5	19.6	4.7
2	50	0.125	0.057	0.456	19.3	19.4	-	5.5
3	51	0.165	0.071	0.430	18.9	19.0	19.1	4.5
4	50	0.205	0.084	0.410	18.6	19.0	-	4.7

D_r = relative density; σ_h at end of consolidation; S = Stroke number.

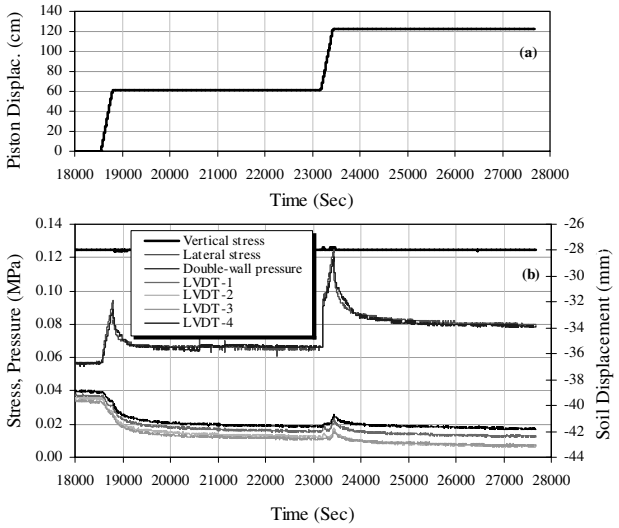

Figure 3. Injection results of Case-2: (a) pump piston displacement; (b) vertical displacement and stresses of soil.

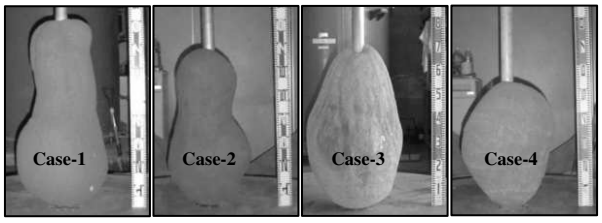

Figure 4. Shapes of injected grout bulbs.

constantly equal to the developed lateral stress. This indicates a proper control of BC3. It should be noted that the vertical displacements measured by the four LVDTs are highly consistent and almost identical. This reveals that the chamber piston was uniformly sliding during injection and suspension.

Figure 4 shows the shapes of the injected grout bulbs. Globular bulbs were formed without penetration into or mixing with the soil. In other words, the injected grout was expanding during injection and displacing the surrounding soil through a distinct grout-soil interface.

4 DEFORMATION MECHANISMS

Figure 5 shows the variation of the vertical displacement (average of those measured by the four LVDTs) of soil surface (δ) with injection for the four cases; δ is significant during and after injection. During suspension and after termination of injection, the soil experienced gradually increasing settlement. Considering that the soil did not experience significant displacement at the lateral boundary (BC3 was imposed) and at the grout-soil interface during suspension (the valve between the pump and the injection pipe was closed after every stroke), it is concluded that this settlement is attributed to the creep deformation of the soil. It should be noted that the soil should have experienced a displacement at the grout-soil interface due to grout consolidation and bleeding. However, this displacement is assumed to be considerably smaller than that due to creep.

During the first stroke, the soil surface was settling. However, during the second and third strokes, it was upheaving or upheaving-settling. By carefully examining the results, it is seen that δ during a given stroke is significantly different from that during the preceding one; the subsequent stroke is associated with smaller settlement and/or larger upheave. This is attributed to the increasing densification of soil due to injection and the creep deformation experienced during suspension. Therefore, it may be said that, with injection, δ due to both injection and the subsequent creep changes gradually from settlement to upheave;

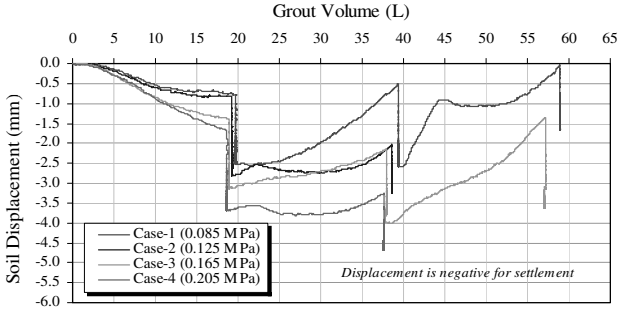

Figure 5. Vertical displacement of soil surface with injection.

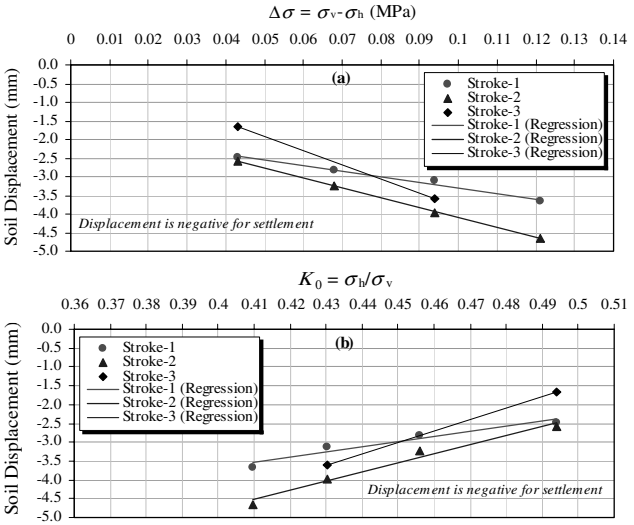

Figure 6. Variation of vertical displacement of soil surface with initial stress state: (a) stress difference $\Delta\sigma$; (b) stress ratio K_0.

with injection the settlement increases at an attenuating rate until reaching a maximum value, and is then followed by upheave which increases at an increasing rate.

The results in Fig. 5 indicate for a given grout volume that the settlement increases and the upheave experienced after the maximum settlement decreases with increasing the vertically confining stress. This variation of settlement may appear unexpected when thinking about the confinement in terms of σ_v only. However, it may be understood by considering the confinement not only in terms of σ_v, but in terms of both σ_v and σ_h, as may be represented by the initial stress difference ($\Delta\sigma = \sigma_v - \sigma_h$) or stress ratio ($K_0 = \sigma_h/\sigma_v$). Figure 6 shows the variation of δ with $\Delta\sigma$ and K_0, for the three strokes. The represented data are those which were measured at the ends of the suspensions or sufficiently after the termination of injection (after reaching equilibrium). Trend lines are also shown. This representation indicates for a given grout volume (or number of strokes) that the settlement increases with increasing $\Delta\sigma$ and decreasing K_0. It also highlights the effect of confinement on the increase of settlement with injection, and reveals that the increase of settlement due to injection of a given grout volume (consider the results of the first and second strokes) increases with increasing $\Delta\sigma$ and decreasing K_0. However, if the injection is continued after reaching the maximum settlement, the upheave due to a given grout volume (consider the results of the second and third strokes) increases with decreasing $\Delta\sigma$ and increasing K_0.

Considering that BC3 was imposed on the soil, the grout did not return in the injection pipe, the change in grout volume due to its consolidation and bleeding is assumed as neglected and the grout did not mix with or penetrate into the soil, the soil volume change (ΔV_s) with injection can be calculated from the corresponding grout volume (V_g) and δ. Figure 7 shows a representation of the volume change ratio (VCR) with injection; VCR = $\Delta V_s/V_g$. It is seen that the volume change due to soil

displacement, ΔV_δ, is significantly large; for instance, the injection of 18.9 and 18.6 L of grout in Cases-3 and 4 resulted in ΔV_δ of as large as 25 and 30% of the corresponding V_g, respectively. It is also seen that the variation of deformation mechanisms with injection affects VCR considerably. The largest VCR was obtained before starting the second stroke (before the upheave onset), then it decreased with continued injection. This decrease is attributed to the increasing contribution of injection to upheave. Figure 7, in addition, shows that ΔV_δ is larger for the soils of higher $\Delta\sigma$ and smaller K_0. The conventional design approach of compaction grouting has been assuming that $\Delta V_s = V_g$. The above discussion and observations indicate however that the soil deformation due to injection and its variation with injection, as well as the soil stress condition, considerably influence the soil volume change and thus the obtained improvement. A reliable design approach should therefore consider the soil stress condition and the grouting-associated soil deformations.

5 COEEFICIENT OF EARTH PRESSURE AT REST (K_0)

As shown in Fig. 3-b, σ_h increases continuously with injection. During suspension, it decreases gradually with time. The residual σ_h is significantly larger than the initial one. It is also seen that immediately after resuming the injection (after suspension) σ_h increases sharply. Then, with continued injection it follows almost the same rate of increase as that of the preceding injection. These observations along with the above ones reveal the significance of the soil rheological properties (in terms of creep deformation and lateral stress relaxation). They also indicate that during the post-suspension injection, in contrary to the developed δ which is significantly influenced by the suspension, the developed σ_h is not significantly influenced.

Figure 8 shows the variation of σ_h with injection for the four cases. It is seen that σ_h increases continuously with injection and that the rate of increase is not the same for all cases. In addition, for a given case, the rate of increase is not constant, but decreases with injection. The residual σ_h increases with the grout volume.

K_0 is an important soil state parameter and is used in evaluating the effectiveness of compaction grouting in solving different problems, such as increasing the liquefaction resistance and the bearing capacity and reducing the soil settlement. Boulanger & Hayden (1995) and Salgado et al. (1997), among others, emphasized the need to investigate and quantify the effects of compaction grouting on K_0.

Since BC3 was imposed on the soil during injection and suspension, the measured σ_h can be considered as a direct measure of K_0, if the vertical stress is considered (K_0 is the ratio of σ_h to σ_v at zero lateral strain). Figure 9 shows the increase of K_0 with injection for the four cases; the increase is represented as K_0–$K_{0(i)}$, where K_0 is the current value, and $K_{0(i)}$ is the initial value (before starting injection). This indicates that K_0–$K_{0(i)}$ has a unique relationship with the grout volume. The rate of increase is attenuating with injection and this is most likely attributed to the increasing contribution of injection to upheave.

6 SUMMARY AND CONCLUSIONS

A physical modeling of compaction grouting using large-scale calibration chamber and injection systems was described in this paper. The results of injections under different confining stresses were also presented and used to discuss the variation of soil displacement and volume change, as well as the lateral stress, with injection. The following conclusions can be made for the soil and conditions considered in the paper.

Compaction grouting induces large vertical displacement in the soil. This displacement changes gradually from settlement to upheave with injection. When injection is suspended, settlement as a result of creep deformation is experienced. The soil volume change due to the vertical displacement is significantly large.

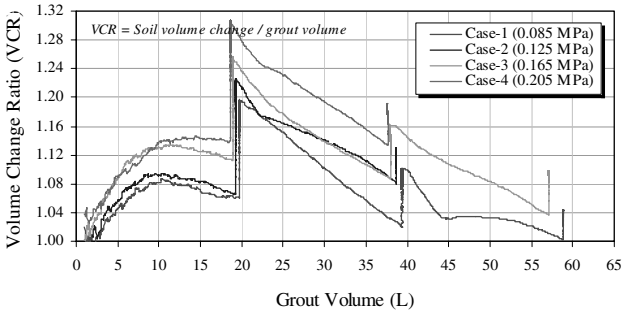

Figure 7. Volume change ratio with injection.

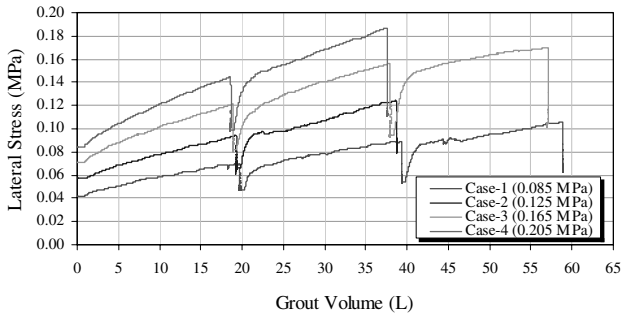

Figure 8. Lateral soil stress with injection.

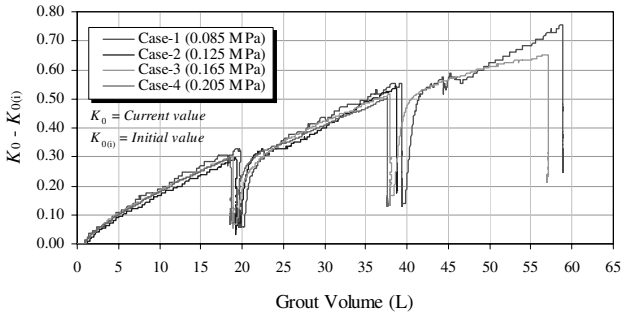

Figure 9. Increase of K_0 with injection.

The initial stress state of soil in terms of $\Delta\sigma$ and K_0 significantly influences the vertical displacement and thus the volume change of soil. The settlement and its increase with injection increase with increasing $\Delta\sigma$ and decreasing K_0. After reaching the maximum settlement, the experienced upheave increases with decreasing $\Delta\sigma$ and increasing K_0.

The lateral stress and K_0 increase continuously with injection. During suspension, the lateral stress experiences relaxation; the residual value is significantly larger than the initial one and increases with the grout volume. The increase of K_0 has a unique relationship with the grout volume.

REFERENCES

Baker, W.H. 1985. Embankment foundation densification by compaction grouting. *Proc., Issues in Dam Grouting,* W.H. Baker, ed., ASCE, New York, N.Y., 104–122.

Boulanger, R.W. & Hayden, R.F. 1995. Aspects of compaction grouting of liquefiable soil. *J. Geotech. Engrg.*, ASCE, 121(12): 844–855.

El-Kelesh, A.M. & Matsui, T. 2008. Calibration chamber modeling of compaction grouting. *Geotech. Testing J.*, 31(4): 295 – 307.

Salgado, R., Boulanger, R.W. & Mitchell, J.K. 1997. Lateral stress effects on CPT liquefaction resistance correlations. *J. Geotech. and Geoenvir. Engrg.*, ASCE, 123(8): 726–735.

Salgado, R., Mitchell, J.K. & Jamiolkowski, M. 1998. Calibration chamber size effects on penetration resistance in sand. *J. Geotech. and Geoenvir. Engrg.*, ASCE, 124(9): 878-888.

Parkin, A.K. & Lunne, T. 1982. Boundary effects in the laboratory calibration of a cone penetrometer in sand. *Proc., Second Europ. Symp. on Penetration Testing*, Amsterdam, 2: 761-768.